

January 01, 2010

The development of a versatile and expeditious route to PET imaging ligands and its potential applications to prostate cancer treatment and diagnosis

Patrick Chow Yuen Ng
Northeastern University

Recommended Citation

Ng, Patrick Chow Yuen, "The development of a versatile and expeditious route to PET imaging ligands and its potential applications to prostate cancer treatment and diagnosis" (2010). *Chemistry Master's Theses*. Paper 13. <http://hdl.handle.net/2047/d20000131>

THE DEVELOPMENT OF A VERSATILE AND EXPEDITIOUS
ROUTE TO PET IMAGING LIGANDS
AND
ITS POTENTIAL APPLICATIONS TO PROSTATE CANCER
TREATMENT AND DIAGNOSIS

A Thesis Presented

By

Patrick Chow Yuen Ng

to

The Department of Chemistry and Chemical Biology

In partial fulfillment of the requirements for the degree of

Master of Science

in the field of

Chemistry

Northeastern University

Boston, Massachusetts

May, 2010

THE DEVELOPMENT OF A VERSATILE AND EXPEDITIOUS
ROUTE TO PET IMAGING LIGANDS
AND
ITS POTENTIAL APPLICATIONS TO PROSTATE CANCER
TREATMENT AND DIAGNOSIS

by

Patrick Chow Yuen Ng

ABSTRACT OF THESIS

Submitted in partial fulfillment of the requirements
for the degree of Master of Science in Chemistry
in the Graduate School of Arts and Sciences of
Northeastern University, May, 2010

ABSTRACT

Chapter 1 of this thesis describes the development of potential PET imaging ligands using microwave thermolysis. Work described in this chapter was primarily investigated at Northeastern University under the supervision of Professor Graham B. Jones. The microwave accelerated fluorodenitration reaction using KF/K222, TBAF/THF (DMSO) and anhydrous TBAF is discussed. The applications of such reactions to commercial pharmaceuticals and potential PET imaging agents are demonstrated. In addition, a novel route to access arenes with a fluoro alkyl tether is explored. The development of the tandem Hiyama coupling fluoro alkylation reaction is discussed.

Chapter 2 delves into potential applications of the expedited fluorination reactions reported in Chapter 1 to prostate cancer. The studies reported in this section took place in the Harvard Medical School/Beth Israel Deaconess Medical Center (HMS/BIDMC) labs under the supervision of Dr. Changmeng Cai and Dr. Steven P. Balk. Chapter 2 describes studies of intratumoral androgen synthesis, a mechanism of androgen receptor (AR) activation in CRPC. The conversion of cholesterol to androgens such as DHT and testosterone occur with the aid of different enzymes. A systematic study of these enzymes and their effects on AR activity is discussed. Data obtained from this study will be used to validate AR as an imaging target and to develop selective imaging agents for PET scanning.

Also at HMS/BIDMC, our group investigated a protein (HIF-1) involved in cell survival, protein synthesis, transcription, cell growth and proliferation. The effects of different drugs such as rapamycin (mTOR inhibitor), metformin (originally anti-diabetic drug), and bicalutamide (anti-androgen) on this protein was studied. The results of these experiments,

will not be described in detail in this thesis, but have played an enormous role in my training and studies related to prostate cancer.

Lastly, I spent six educational months working at Novartis Pharmaceuticals. I was working on developing the SAR of potential broad spectrum antibiotics. The details of this project cannot be discussed at this time.

ACKNOWLEDGEMENTS

First and foremost, I would like to thank my family, particularly my parents, Dr. and Mrs. Phick H. Ng for their love, support, guidance and understanding; especially during the stressful times of my academic career. None of my accomplishments, both personal and academic, would have been possible without them, and for this I am truly grateful.

I would like to thank my friends for their support and role in my development both intellectually and socially.

Special thanks to Professor Graham B. Jones and the Jones group at Northeastern University for their support and guidance throughout my academic career. Despite his busy schedule, Professor Jones always took the time to support me in my endeavors and guide me in my work. Additionally, Professor Jones has directed me to his collaborators to help me gain experience in other fields to develop my interest in medicine.

Lastly, I would like to express my gratitude to Dr. Changmeng Cai, Dr. Shaoyong Chen, Dr. Steven Balk and Dr. Glenn Bublely of Harvard Medical School/Beth Israel Deaconess Medical Center for all their support and guidance. Working and interacting with them has truly been an inspiring and motivation experience.

TABLE OF CONTENTS

Abstract	2
Acknowledgements	5
Table of Contents	6
List Of Figures, Schemes and Tables	7
Chapter 1: Development of the Microwave Accelerated Fluorodenitration Reaction and the Introduction of the Tandem Hiyama Coupling Fluoroalkylation Reaction	9
1.1 Introduction and Background	10
1.2 Experimental	18
1.3 Results/Discussion	19
1.4 Future Directions	30
References	32
Chapter 2: The Study of Androgen Synthesis and Potential PET imaging Ligands for Prostate Cancer	34
2.1 Introduction and Background	35
2.2 Experimental	41
2.3 Results/Discussion	43
2.4 Future Directions	57
References	64

LIST OF FIGURES SCHEMES AND TABLES

Figure 1.1: Structure of K222 Kryptofix and the formation of side products using A: KF/K222 System and B: reagent grade TBAF/THF	13
Figure 1.2: Fluorodenitration Reactions of Various Arenes	15
Scheme 1.1: Synthesis of Haloperidol via Microwave Accelerated Fluorodenitration	16
Figure 1.3: Commercial pharmaceuticals containing fluoroarene	17
Table 1.1/Scheme 1.2: Tandem Hiyama Coupling Fluorination Reaction Using PdI ₂	20
Table 1.2/Scheme 1.3: Tandem Hiyama Coupling Fluorination Reaction Using Pd(OAc) ₂	21
Table 1.3/Scheme 1.4: Tandem Hiyama Coupling Fluorination Reaction Using PdBr ₂	22
Table 1.4: Varying Catalytic Presence at Optimal Temperature and Hold Time	23
Figure 1.4: Generic Hiyama Coupling Reaction Mechanism	27
Scheme 1.5: Formation of Alcohol Side Products	29
Figure 2.1: Fluorolabeled Androgen Derivatives	39
Figure 2.2: Androgen Synthesis Pathway	40
Figure 2.3: Treatment of PCa cell line expressing mutant AR with various androgens	44
Figure 2.4: mRNA studies of CYP11A1 and CYP17A1 Enzymes in Metastatic CRPC cells	46
Figure 2.5: mRNA Expression of Proteins Involved in Androgen Synthesis	50
Figure 2.6 : Comparison of CYP11A1 Protein Levels in Different Cell Lines	51
Figure 2.7: Structures for CYP17A1 Inhibitors Abiraterone and Ketoconazole	52
Figure 2.8: Western Blot of C4-2 Cells treated with Abiraterone and Progesterone for 24 hours	53
Figure 2.9: Western Blot of C4-2 Cells Treated with DHT, Ketoconazole and Abiraterone for 24 hrs	54
Figure 2.10: Preliminary siRNA CYP11A1 experiment	55

Figure 2.10b: Luciferase Assay Comparing Androgen Induced activity of Wild-Type(WT) and Mutant AR and the Effects of Abiraterone	56
Figure 2.11: Indomethacin, non-steroidal anti-inflammatory drug (NSAID) shown to have inhibitory effects on AKR1C3 in PCa	58
Figure 2.12: Combination Treatment of Abiraterone and Indomethacin	59
Scheme 2.1: Potential Synthetic Route to Fluorolabeled Androgen	62
Scheme 2.2: Possible Expedited Route to non-androgenic Fluorolabeled PCa Imaging Ligands (Flutamide derivatives)	63

Chapter 1:
Development of the Microwave Accelerated Fluorodenitration Reaction
and
the Introduction of the Tandem Hiyama Coupling Fluoroalkylation Reaction

1.1: Introduction and Background

For PET imaging, the past decade has seen numerous improvements. The development of positron emission tomography (PET) scanning continues as a rapidly growing area of research¹⁰. It remains a unique and noninvasive tool in its medical and pharmacological applications. This method of imaging uses the properties of radio-labeled compounds. Such compounds contain a neutron-deficient positron (e^+) emitting isotope. The radio-labeled molecular probes are intravenously administered to a host; the host then metabolizes the compound, and the positron emissions from the radio-label are detected via scintillation detectors and the data is stored in sinograms. Then, using mathematical algorithms, the data is translated into a three dimensional image¹³. Unlike more traditional scanning methods such as X-rays and CT scans, PET imaging provides both metabolic as well as anatomical data. As a result, PET imaging has unique and important applications in pharmacology and in the study of different conditions such as metastatic cancer and neurodegenerative diseases like Alzheimers^{1,11}.

Tumor detection and CNS imaging currently employ the use of 2-[¹⁸F] fluoro-2-deoxy-D-glucose (FDG). FDG remains the most widely used tracer in PET imaging^{10,15,17}. FDG is metabolized in vivo and concentrates itself in certain parts of the body characterized by high metabolism. Such areas can consist of malignant cells like those that compose tumors. Images are produced and can be used to distinguish areas of abnormal metabolic activity from areas that have normal activity. Such information provides valuable data in assessing and diagnosing different conditions⁶.

In the early 21st century, major clinical limitations of PET imaging included lengthy scan times, high expenses and inaccurate image translation due to detector limitations. Over the past few years, however, improvement in detector techniques has revolutionized PET imaging. With new scintillation detectors and new image reconstruction techniques, high resolution images are realized in less than 10 minutes¹³. With the increase in PET imaging applications, the technique has become a reimbursable clinical procedure, and is rapidly moving towards being routine in the assessment of various diseases.

Despite these improvements, molecular probes used in the scan, such as FDG, continue to exhibit several limitations⁶. For example, FDG remains as an unspecific radiotracer, meaning that it does not have a particular anatomical target. As a result, any cell which metabolizes glucose will have FDG uptake. Organ systems including the liver or bladder, which are characterized by high blood flow, naturally have a high uptake of FDG. Thus tumors or abnormalities in such regions may remain undetected due to the high background realized with these organ systems¹⁵. Thus, the need for different, more specific radiotracers is apparent.

The development of such radiotracers has been explored using various radioisotopes including but not limited to ¹¹C, ¹³N, ¹⁵O, and ¹⁸F, with respective half-lives of 2, 10, 20, and 119 minutes⁵. The short half-lives of these radioisotopes pose a limitation in the synthesis of radioactive compounds for PET imaging. Of the isotopes mentioned, ¹⁸F serves as an attractive candidate in the synthesis of PET imaging ligands with its longer half-life and its important role in improving the efficacy and potency of commercial pharmaceuticals as demonstrated in Atorvastatin and Ciprofloxacin^{2,3} (Figure 1). However, 119 minutes is not much time to work with when synthesizing, purifying and administering a radioactive compound.

The microwave expedited fluorodenitration reaction comes to mind when thinking about this area. This reaction and its applications to various substituted arenes and commercial compounds has been studied by our group^{3,5}. Preliminary studies were done using KF/K222 Kryptofix (K222, 4, 7, 13, 16, 21, 24-Hexaoxa-1, 10-diazabicyclo [8.8.8]-hexacosane) as a fluorine source/phase transfer catalyst. Various reaction conditions using microwave thermolysis were tested. It was found that a strong electron withdrawing group (CHO) was needed in the ortho position of the nitro arene for the reaction to occur. Relocation of the EWG as demonstrated with the use of p-nitrobenzaldehyde resulted in no product formation. As a major side product, biarylether was formed via nucleophilic denitration by phenoxide formed *in situ*³. In addition to these issues, the high cost of K222 (Approximately \$100/gram¹⁶) further contributed to the disadvantages associated with this reaction. With the limited success of these preliminary experiments, it became evident that this would not provide a versatile and efficient approach to synthesize a variety of radiotracers for PET imaging. An approach to prevent phenoxide from forming would be to trap the nitrite ion *in situ*. However, this would add to reaction time as well as add steps to work up. As a result, a more nucleophilic source of fluorine was investigated^{3,5}.

The fluorodenitration reaction was further explored using tetra-n-butylammonium fluoride (TBAF) in this reaction. TBAF was attractive as it would serve a dual role as a fluorine source and phase transfer catalyst. Varying the reaction conditions and the identity of the substituted arenes was done to investigate this reaction. Previously, the fluorodenitration of substituted pyridine rings was explored. Kuduk et al. reports efficient conversion of 2- and 4-nitropyridines to target fluoroarene at mild temperatures using TBAF. However the need for an electron withdrawing group was apparent with nitropyridines.

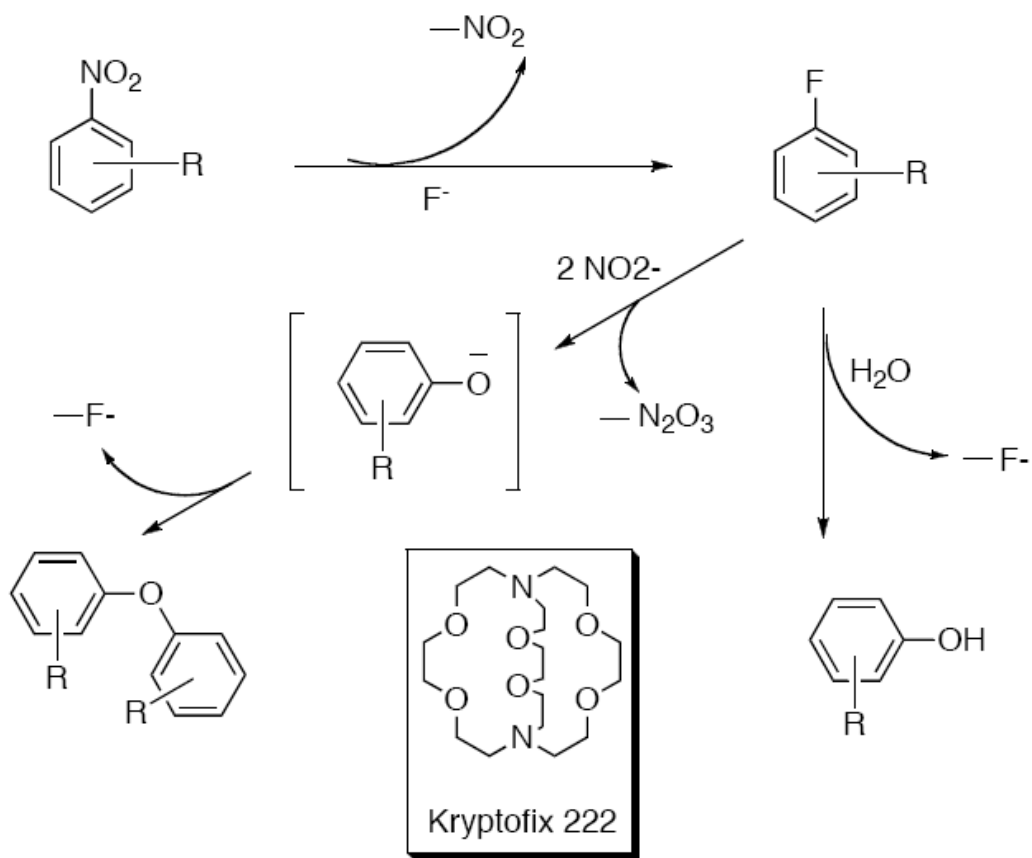


Figure 1.1: Structure of K222 Kryptofix and the formation of side products using A: KF/K222

System and B: reagent grade TBAF/THF

In our experiments, excellent yields of target fluoroarene were observed when using compounds such as p-nitrobenzyl cyanide. Minimal yields were observed when using arenes such as 1-nitro-4-trifluoromethyl benzene and p-nitrobenzaldehyde. Furthermore, applications to nitro pyridines were severely limited⁵. The formation of biaryl ether was not observed with the use TBAF. However, despite practicing anhydrous technique, substantial conversion to phenolic derivatives was observed due to the presence of water in reagent grade TBAF (5% water by volume)^{3,5,16}.

As a solution to this problem, anhydrous TBAF was prepared in situ via TBACN/hexafluorobenzene exchange¹². Anhydrous TBAF was used for fluorodenitration reactions. Consistent and high conversions of target fluoroarene were observed with the use of a variety of arenes (Figure 1.2), and applications were demonstrated with the microwave accelerated synthesis of Haloperidol (Scheme 1.1) and Risperidone (Figure 1.3)⁵.

With the fluorodenitration reaction explored, the need of other options in the accelerated synthesis of fluorolabeled compounds became of interest. Presented in this chapter is another potential synthetic route to fluorolabeled compounds. A novel method using microwave themolysis to alkylate and fluorinate an arene ring in tandem was investigated³. High conversion to target fluoroalkylated arene was achieved in less than 5 minutes.

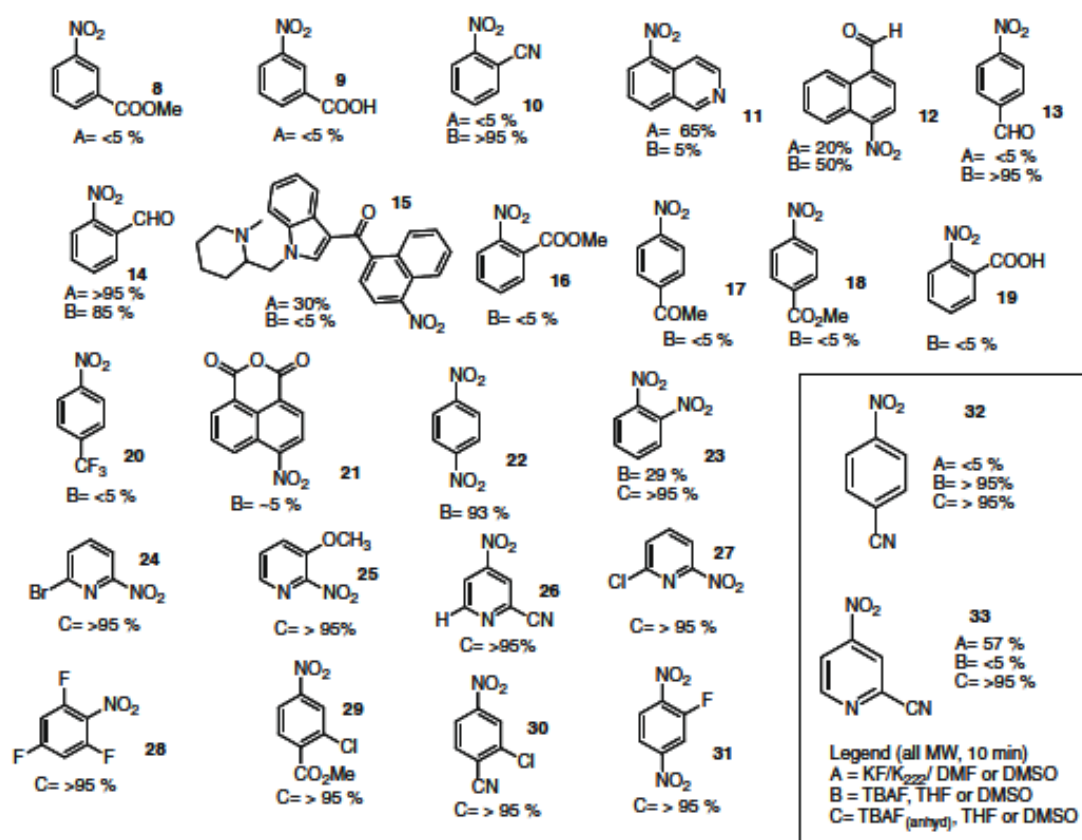
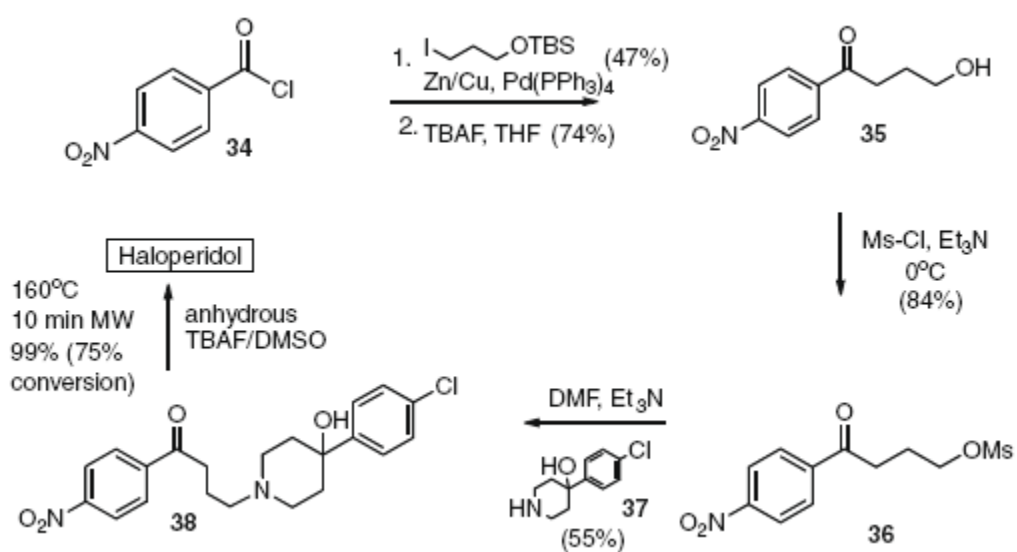


Figure 1.2: Fluorodenitration Reactions of Various Arenes (LaBeaume et al.)



Scheme 1.1: Synthesis of Haloperidol via Microwave Accelerated Fluorodenitration

(LaBeaume et al.)

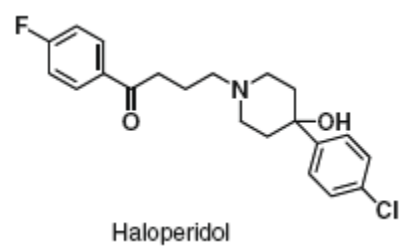
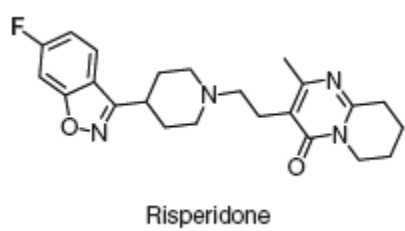
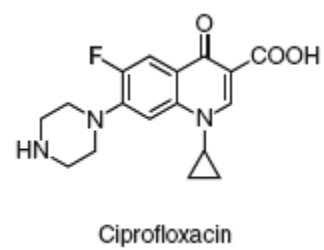
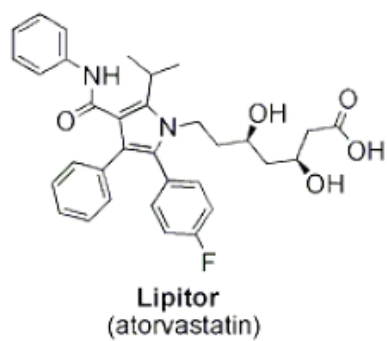


Figure 1.3: Commercial pharmaceuticals containing fluoroarene

1.2: Experimental

All reactions were conducted in a CEM brand Discover microwave reactor. Reactions were conducted at 300 watts, 250 PSI and a run-time of 5 minutes. Hold time, temperature, and catalyst system were varied. Solvent was purchased from Aldrich in Sure Seal bottles and handled using anhydrous technique. All reagents were commercially available with the exception of the alkylbromotosylates which were prepared via tosylation of the respective bromo alcohols. Chemical yields and percent conversions were determined using GC-MS (Supelco SPB 624 volatile column (length: 60.0m, diameter: 250um, film thickness: 1.4um)). Run was characterized by 40-250°C ramp in temperature at a rate of 10°C/min with initial hold time of two minutes and final hold time of five minutes. (Method was developed by Matthew Daniels, BS/MS' 2007.)³

General Procedure for the Preparation of Fluoroalkylated Arenes:

In a dry CEM brand microwave tube with magnetic stir bar, the respective silylarene (1.2mmol), phosphonium salt (.1mmol) and palladium catalyst (.04mmol) was dissolved in 1.2mL THF and 50uL TBAF(1M solution in THF). Solution was allowed to stir at room temperature (RT) for 30 minutes during which a brilliant golden color was realized. After 30 minutes, tetra-n-butylammonium fluoride (3.6mL of 1M solution in THF) and 1.5eq. of alkylbromotosylate was added to reaction mixture. Vial was placed in microwave reactor and heated to 80°C for 2 minutes. Vial was allowed to cool to room temperature. Mixture was diluted with deionized water and extracted 3x with ethyl acetate through silica plug. Organics were

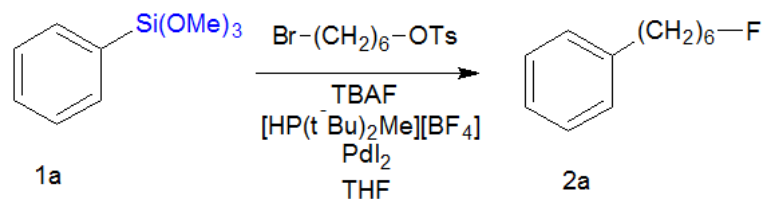
washed with 10% HCl(1x) and with brine (1x). Organic layer was analyzed via GC-MS and quantified using 1 equivalent of octane as an internal standard.

1.3: Results/Discussion

All peaks were identified using GC/MS system. Retention time for 1-fluoro-6-phenyl hexane was determined to be 24.36 minutes. Peaks at m/z 180 and 91 were characteristic of the product. Percent conversion was determined by comparing the area of the peaks of the octane internal standard and the area of the product peak at 24.36 minutes. Areas were determined using software on computer. Side products were identified using library scan.

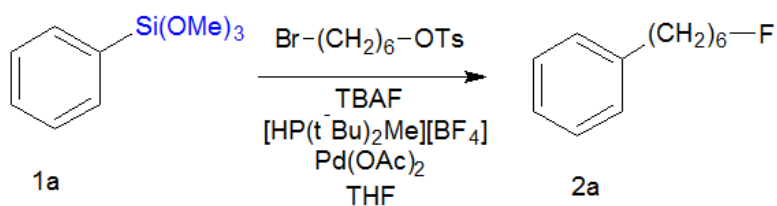
The goal of this area of the project was to expand the routes of fluorinating different arene rings. With the fluorodenitration reaction optimized, the route to alkylating and fluorinating an arene in tandem was explored using different microwave conditions and palladium catalyst systems (Scheme 1.2- Scheme 1.4).

The role of a fluorine moiety in different commercial pharmaceuticals is monumental in improving potency and efficacy of the molecule². As described earlier, our group has extensively explored the microwave accelerated fluorodenitration reactions of various substituted arene rings using KF/K222, TBAF/THF (DMSO) and TBAF (anhy)/THF (DMSO)^{3,5}. With the application of this methodology to Haloperidol and other fluorine labeled pharmaceuticals, we decided to explore a reaction that would provide another route to introduce fluorine into an arene in

Scheme 1.2: Tandem Hiyama Coupling Fluorination Reaction Using PdI₂

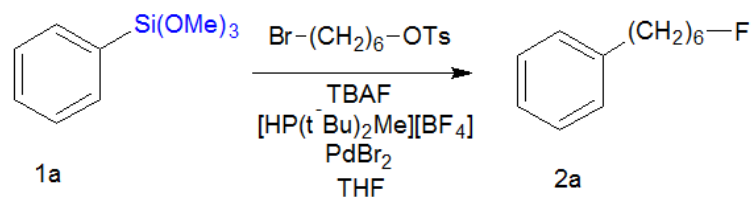
Entry	Catalyst System	Temperature °C	Hold Time(min)	Yield
1	PdI ₂ /[HP(t-Bu) ₂ Me][BF ₄]	60	2	24
2	PdI ₂ /[HP(t-Bu) ₂ Me][BF ₄]	70	2	25
3	PdI ₂ /[HP(t-Bu) ₂ Me][BF ₄]	80	2	25
4	PdI ₂ /[HP(t-Bu) ₂ Me][BF ₄]	85	2	27
5	PdI ₂ /[HP(t-Bu) ₂ Me][BF ₄]	90	2	15
6	PdI ₂ /[HP(t-Bu) ₂ Me][BF ₄]	100	2	12
7	PdI ₂ /[HP(t-Bu) ₂ Me][BF ₄]	110	2	9

Table 1.1

Scheme 1.3: Tandem Hiyama Coupling Fluorination Reaction Using Pd(OAc)₂

Entry	Catalyst System	Temperature °C	Hold Time(min)	Yield
1	Pd(OAc) ₂ /[HP(t-Bu) ₂ Me][BF ₄]	60	2	26
2	Pd(OAc) ₂ /[HP(t-Bu) ₂ Me][BF ₄]	70	2	25
3	Pd(OAc) ₂ /[HP(t-Bu) ₂ Me][BF ₄]	80	2	27
4	Pd(OAc) ₂ /[HP(t-Bu) ₂ Me][BF ₄]	85	2	24
5	Pd(OAc) ₂ /[HP(t-Bu) ₂ Me][BF ₄]	90	2	21
6	Pd(OAc) ₂ /[HP(t-Bu) ₂ Me][BF ₄]	100	2	13
7	Pd(OAc) ₂ /[HP(t-Bu) ₂ Me][BF ₄]	110	2	9

Table 1.2

Scheme 1.4: Tandem Hiyama Coupling Fluorination Reaction Using PdBr₂

Entry	Catalyst System	Temperature °C	Hold Time(min)	Yield
1	PdBr ₂ /[HP(t-Bu) ₂ Me][BF ₄]	60	2	51
2	PdBr ₂ /[HP(t-Bu) ₂ Me][BF ₄]	70	2	55
3	PdBr ₂ /[HP(t-Bu) ₂ Me][BF ₄]	80	2	61
4	PdBr ₂ /[HP(t-Bu) ₂ Me][BF ₄]	85	2	48
5	PdBr ₂ /[HP(t-Bu) ₂ Me][BF ₄]	90	2	45
6	PdBr ₂ /[HP(t-Bu) ₂ Me][BF ₄]	100	2	42
7	PdBr ₂ /[HP(t-Bu) ₂ Me][BF ₄]	110	2	14

Table 1.3

Varying Catalytic Presence at Optimal Temperature and Hold Time

Entry	Catalyst System	Eq. Catalyst	Temperature °C	Hold Time(min)	Yield
1	PdI ₂ /[HP(t-Bu) ₂ Me][BF ₄]	.14	80	2	27
2	PdI ₂ /[HP(t-Bu) ₂ Me][BF ₄]	.24	80	2	33
3	PdI ₂ /[HP(t-Bu) ₂ Me][BF ₄]	.34	80	2	54
4	Pd(OAc) ₂ /[HP(t-Bu) ₂ Me][BF ₄]	.14	85	2	27
5	Pd(OAc) ₂ /[HP(t-Bu) ₂ Me][BF ₄]	.24	85	2	33
6	Pd(OAc) ₂ /[HP(t-Bu) ₂ Me][BF ₄]	.34	85	2	42
7	PdBr ₂ /[HP(t-Bu) ₂ Me][BF ₄]	.14	80	2	61
8	PdBr ₂ /[HP(t-Bu) ₂ Me][BF ₄]	.24	80	2	76
9	PdBr ₂ /[HP(t-Bu) ₂ Me][BF ₄]	.34	80	2	81

Table 1.4

minimal time. An accelerated methodology to introduce a fluoroalkyl tether to an arene ring was explored. Exploration of the tandem Hiyama Coupling reaction shows a dependence on the temperature, hold-time and amount of catalyst present.

With the guidance of data presented by Fu et al., the Hiyama Coupling reaction was first explored using alkyl bromides and iodides for coupling. Fu reports modest to excellent yields in the coupling of unactivated alkyl bromides and iodides via palladium catalyzed Hiyama Coupling with the use of air and moisture-stable phosphonium salts⁷. In our experiments, the alkyl halides were prepared from their respective alcohols. The coupling of the tosyl alkyl iodide to arene resulted in poor yields, resulting in substantial amounts of unreacted starting material. Upon examination of this reaction, it was found that the low conversion of starting material was due to the formation of the difluoro-alkyl compound. Fluorine nucleophilically displaced both the tosylate and the iodine from the alkyl chain, preventing the progression of the coupling reaction.

With this in mind, our group decided to explore the use of the tosyl alkyl bromides. Fortunately, we found that this reaction proceeded with minimal debromination of the starting material. Using the alkyl bromide, the tandem coupling reaction was explored very systematically. First, various commercially available palladium ligands were purchased. The first reactions tested are summarized in Table 1.1. Various temperatures and hold-times were explored and the reaction using this system was optimized at conditions summarized in Table 1.1 entry 4. A similar approach was taken using the different palladium ligands as seen in Tables 1.2 and 1.3. A potential problem that we expected was reported by Zhang et. al. who reports high conversion to target biaryl compounds by coupling arenesulfonates with aryl silanes. These

reactions resulted in the displacement of the tosyl group on the arenesulfonates. Coupling of the alkyl chain at the tosylate end was not observed in our experiments indicating that the rate of tosyl displacement of the bromotosylates is significantly higher compared to the coupling reaction in these experiments.

The most promising results were seen when using the PdBr₂ ligand reported in Table 1.3. The drastic difference in yields using these different ligands can be partially attributed to the sterics of the ligand. Pd(OAc)₂ and PdI₂ are substantially larger compared to PdBr₂. These more sterically hindered catalysts may react at a slower rate, specifically at the oxidative insertion step of the reaction mechanism (Figure 1.4). This results in less conversion of starting material in the given time. Having observed the dependence of this reaction on the catalytic system, we decided to vary the amount of catalyst in the system. As summarized in Table 1.4, increasing the catalyst has a direct correlation with the conversion to product 2a. Given these conditions, the reaction was optimized at 80°C, 2 minutes with .34eq of PdBr₂/ [HP(t-Bu)₂Me][BF₄] present in the reaction.

Upon further analysis of this reaction mechanism, a few concerns arise. The primary and most obvious issue is the need for an excessive amount of catalyst to achieve good to excellent yields. The use of .34eq of a catalyst system is virtually unheard of in published, optimized cross coupling methods. Additionally, catalyst compounds are quite expensive¹⁶, and the use of such an excessive amount in this system demonstrates the need for further exploration and optimization of this reaction. For those reactions with <50% yield to 2a, conversion to phenol (2b) and 6-phenyl alcohol (2c) was observed (Scheme 1.5). Although anhydrous technique was employed in these reactions, the presence of H₂O (5% by weight) in reagent grade TBAF may be

responsible for these side products. Conversion to 2b and 2c was seen with reactions at lower temperatures (eg. $<80^{\circ}\text{C}$). At higher temperatures ($>95^{\circ}\text{C}$), the side products were unidentifiable. GC-MS spectra became more ambiguous with extraneous peaks indicating decomposition of the starting material and/or product when the temperature was increased. In some cases, the traces of benzene were observed as a side product. Additionally, at higher temperatures, a black sludge with a terrible smell was realized upon completion of the reaction. Although some product was observed in these reactions (entries 5-7 in Tables 1.1, 1.2, and 1.3) the unidentifiable peaks were indicative of conditions too harsh for optimal conversion to the targeted fluoroalkylarene.

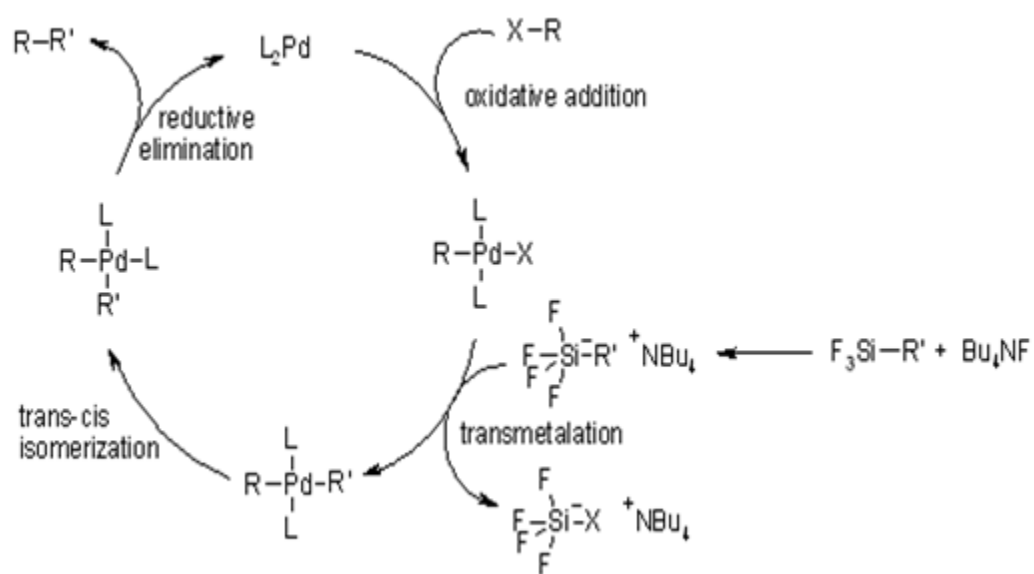
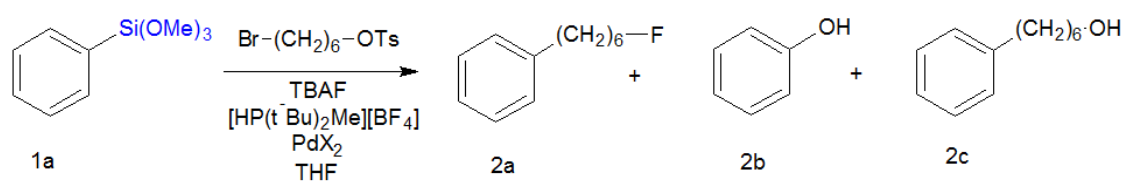


Figure 1.4: Generic Hiyama Coupling Reaction Mechanism^{4,29}

Isolation of compound 2a proved to be unsuccessful despite conversion seen in GC-MS analysis. Product is believed to be volatile and lost when the use silica gel column chromatography was employed. Additionally, scale ups of the reactions were unsuccessful, most likely due to the limitations of the microwave vessel used. Attempts at scale up resulted in aborted runs due to high pressures realized during microwave heating.

The experiments above provide some insight to a possible expedited route to fluoro alkylated arenes. In <5 minutes, excellent yields of 2a were observed using PdBr₂ catalysis and conditions specified in Table 1.3, entry 4.



Scheme 1.5: Formation of Alcohol Side Products

1.4: Future Directions

This preliminary work provides us with a small window into a versatile approach to produce fluoroalkylated arenes. First, the main issue that needs to be addressed is the substantial conversion to the alcohol side products. Water present in the reaction mixture needs to be eliminated. A possible route to explore is to use anhydrous TBAF as the source of fluorine. Similar phenolic side products were observed when the fluorodenitration reaction was explored by our group^{3,5}. The problem was solved with the use of freshly prepared anhydrous TBAF. With the use of anhydrous TBAF in this tandem reaction, more efficient and clean conversions may be observed.

Upon optimization of this reaction, applications to substituted arenes should be investigated. As with the fluorodenitration reaction, the effects of different substituents and heteroatoms, in many cases, are drastic. Preliminary reactions should be conducted using the aldehyde or aniline silyl arenes. It is expected that the influence of such groups will have a minimal effect in the progress of this coupling reaction when compared to the fluorodenitration reaction because of the differences in the mechanisms involved. In the fluorodenitration reaction, the electron withdrawing groups present in the starting material stabilized the anion intermediate formed upon the displacement of the nitro group. Such an anionic intermediate is not formed in the coupling reaction which proceeds through the polarization of the trimethoxysilyl group by fluorine atoms from TBAF. However, to have any potential clinical applications, this reaction must demonstrate good to excellent yields in different heterocycles and substituted arenes.

In addition, shorter alkyl chains should be explored. The six carbon alkyl tethers used in the above experiments may have drastic effects on the chemical properties of different commercial compounds that could potentially be labeled. The use of a smaller tether may prove to better conserve the chemistry of such molecules and may be more cost efficient as well. Furthermore, to improve chemical yields, the effects of the phosphine ligand should be evaluated. Fu et al. describes the sensitivity of the coupling reaction to the size of the R groups in the ligand. Exploration of various PR_3 ligands may prove to be valuable in optimizing this reaction.

Lastly, an application of the fluorodenitration reaction to molecules related to prostate cancer is of interest. The diagnosis and treatment of metastatic prostate cancer is in need of improvement. PET applications for such a disease are limited due to inconsistent results when using different radiolabeled tracers⁶. In order to apply our methodology to develop more accurate and specific radiotracer for prostate cancer, the biochemistry of the disease will be investigated. Chapter 2 delves into our studies of prostate cancer, and the potential imaging agents that may be synthesized.

References:

1. Besson, J.A.; Crawford, J.R.; Evans, N.T.; Gemmell, H.G.; Roeda, D. PET Imaging in Alzheimer's Disease, *J.R. Soc. Med.* **1992**, 85(4): 231-234
2. Chambers, R. D. Fluorine in Organic Chemistry; Blackwell: Oxford, 2005.
3. Daniels, M. *Development of Synthetic Methodology Using Nucleophilic and Electrophilic Fluorine*, **2007**.
4. Hatanaka, Y.; Hiyama, T. Cross Coupling of Organosilanes With Organic Halides Mediated by Palladium Catalyst. *J. Org. Chem.* **1988**, 53: 918-920
5. LaBeaume, P.; Placzek, M.; Daniels, M.; Kendrick, I.; Ng, P.; McNeel, M.; Afroze, R.; Alexander, A.; Thomas, R.; Kallmerten, A.E.; Jones, G.B. Microwave-accelerated fluorordenitrations and nitrodehalogenations: expeditious routes to labeled PET ligands and fluoropharmaceuticals, *Tetrahedron Letters*, **2010**, 51: 1906-19
6. Larson, S.M.; Morris, M.; Guther, I.; Beattie, B.; Humm, J.L.; Akhurst, T.A.; Finn, R.D.; Erdi, Y.; Pentlow, K.; Dyke, J.; Squire, O.; Bornmann, W.; McCarthy, T.; Welch, M.; Scher, H. Tumor Localization of $^{16}\beta$ - ^{18}F -5 α -Dihydrotestosterone Versus ^{18}F -FDG in Patients with Progressive, Metastatic Prostate Cancer, *The Journal of Nuclear Medicine*, **2004**, 45(3): 366-373
7. Lee, J-Y.; Fu, G.C.,; Room-Temperature Hiyama Cross Couplings of Arylsilanes with Alkyl Bromides and Iodides, *J. Am. Chem. Soc.* **2003**, 125: 5616-5617
8. Kuduk S.D.;DiPardo R.M.; Bock M.G. Tetrabutylammonium Salt Induced Denitration of Nitropyridines: Synthesis of Fluoro-, Hydroxy-, and Methoxypyridines, *Organic Letters*; **2005**, 7(4): 577-579
9. Ojima, I. *Fluorine in Medicinal Chemistry and Chemical Biology*, Wiley-Blackwell Inc. Chichester, **2009**
10. Saha, G.B. *Basics of PET imaging*. Springer Science, 2004
11. Salmon, E.; Sadzot, B.; Maquet, P.; Degueldre, C.; Lemaire, C.; Rigo, P.; Comar, D.; Franck,G. Differential Diagnosis of Alzheimer's Disease with PET, *The Journal of Nuclear Medicine*, **1994**, 35(3): 391-398

12. Sun, H.; DiMugno, S.G. Anhydrous Tetrabutylammonium Fluoride. *Journal of the American Chemical Society*; **2005** 127(7): 2050-2051
13. Townsend, DW. Physical Principles and Technology of Clinical PET Imaging. *Ann Acad Med Singapore*; **2004**, 33:133-45
14. Vorogushin, A.V.; Huang, X.; Buchwald, S.L. Use of Tunable Ligands Allows for Intermolecular Pd- Catalyzed C-O Bond Formation. *J. Am. Chem. Soc.* **2005**, 127: 8146-8149
15. Webber, WA PET for Response Assessment in Oncology: Radiotherapy and Chemotherapy. *The British Institute of Radiology*; **2005**, 28: 42-49
16. www.sigma-aldrich.com
17. Yu, S. Review of F-FDG Synthesis and Quality Control. *Biomedical Imaging and Intervention Journal*; **2006**, 2(4),e37
18. Zhang, L.; Wu, J. Palladium-Catalyzed Hiyama Cross-Couplings of Aryl Arenesulfonates with Arylsilanes. *J. Am. Chem. Soc.* **2008**, 130: 12250-12251

Chapter 2:

The Study of Androgen Synthesis and Potential PET imaging Ligands for Prostate Cancer

2.1: Introduction and Background

Prostate cancer remains as the second most common cause of cancer related deaths in males in the United States¹⁴. According to the CDC; 203, 415 men developed prostate cancer and 28, 372 died due to the disease in 2006. The risk of getting prostate cancer increases with age. Over 60% of prostate cancer diagnoses are in males over the age of 60. African-Americans are diagnosed with prostate cancer more than men of any other race. Prostate cancer is least seen in Asian and Hispanic American men. Additionally, men whose diets are rich in dairy fat and red meats have a slight increase in risk of the disease. Other factors such as obesity, exercise, vasectomy and infection have been shown, in some cases, to increase risk of prostate cancer, however these factors are not well studied (ACS, 2009).

The diagnosis of prostate cancer is reached with the help several methods. A digital rectal exam (DRE) is a method involving palpation of the prostate gland through the rectum. The clinician examines for any abnormal growths on or enlargement of the prostates with this exam. Less invasively, prostate-specific antigen levels (PSA) are determined via blood test²⁵. PSA is a gene regulated by the androgen receptor (AR) and is secreted by epithelial cells of the prostate. The androgen receptor plays a vital role in the development of the male sexual phenotype. AR is a nuclear receptor (NR3C4) and is activated by various agonists such as androgens including testosterone and DHT²⁷. Structurally, AR consists of five domains including the N-terminal domain, the ligand binding domain, the DNA binding domain, the hinge domain, and the C-terminal domain²⁷. To achieve AR activation, agonists interact with the ligand binding domain of AR and the receptor undergoes a conformational change. The hinge domain closes the binding pocket securing the agonist in place. AR then migrates to the cell nucleus where it initiates the

transcription of various AR regulated genes like PSA. Prostate cancer patients typically exhibit elevated levels of PSA but a high level of PSA is not always indicative of prostate cancer^{1,19,25}.

When detected in its early stages, prostate cancer is treated using androgen deprivation therapy (ADT). Early stage prostate cancer has been shown to be dependent on androgens such as DHT and testosterone. ADT can be achieved in several ways including chemical and surgical castration. These procedures cause serum levels of androgens to decrease significantly, thus starving the cancer of androgens. Patients have been shown to respond well to ADT. Steep decreases in PSA, a decrease in patient discomfort as well as a decrease in tumor proliferation is usually observed within the first month after treatment^{2,3}. However, within approximately 18 months; a reoccurrence of the cancer is seen. The cancer progresses to a stage called Castration Resistant Prostate Cancer (CRPC) where it metastasizes and most often leads to patient mortality^{2,3,23}. CRPC does not respond well to ADT. Initial responses of CRPC are observed with chemotherapy, however the effects are limited. CRPC generally results in mortality within 9-12 months⁸.

The mechanisms of progression of prostate cancer from early stages to castration resistant stages remain ambiguous. Reports indicate that the progression of prostate cancer can be attributed to one or a combination of the following: AR hypersensitivity, where AR becomes activated with minimal levels of androgens; AR amplification, where genes that encode AR are amplified; AR upregulation, where there is an increase in AR protein levels within the cells; AR mutations, where mutant receptors become activated by other molecules that resemble DHT and testosterone, and intratumoral androgen synthesis, where cells are independently synthesizing and supplying the cancer with androgens^{5,23}. The literature describes several experiments that

support the intratumoral androgen synthesis mechanism. For example, Montgomery et al. reports the presence of sufficient levels of androgens for AR activation in primary prostate tissues in patients who have been treated with medical or surgical castration. Additionally, the group reports prostate cancer proliferation in environments starved of adrenal androgens in xenograft models. Levels of androgens present in prostate cancer cells were significantly higher compared to levels present in other tissue samples obtained from other organs. Additionally, the literature consistently reports an upregulation and amplification of AR in CRPC^{2,3,5,6}.

In combination with a higher AR level, the androgens produced de novo are believed to be sufficient to bind to AR and increase AR activity. Androgens such as DHT and testosterone have been extensively studied in this field and are known to have a high affinity to the androgen receptor¹⁻⁶. Due to their high affinity to AR, DHT and testosterone have been radiolabeled for imaging purposes^{17,18}. Tritium and iodine derivatives of DHT and testosterone have been synthesized¹¹. Additionally, bromine-77 has been used in radiolabeling androgens⁷. However, these reports discuss low affinity and uptake of radio tracers by the AR target. Furthermore, high background was observed due to dehalogenation of the synthesized radiotracers.

More recently, fluorine became of interest in radiolabeling androgens. Liu et. al. reports the successful synthesis of several fluorine-substituted androgens seen in Figure 2.1. Metabolic studies have shown selective uptake in the prostate cancer cells of rat models. However, some molecules, such as fluoro-testosterone (¹⁸FT) and fluoro-dihydrotestosterone(¹⁸FDHT), were metabolized and resulted in defluorination. This caused a high uptake in bone tissue causing background, which, if occurred clinically, would cloud skeletal metastatic tissue images. Derivatives of ¹⁸F-DHT and ¹⁸F-T were synthesized to improve metabolic stability of the

molecule as seen with ^{18}F -MDHT and F-R 1881(Figure 2.1). These molecules proved to be more stable and showed specific uptake in certain lesions. As mentioned in Chapter 1, the main radiotracer used in PET imaging studies is ^{18}F -FDG. As a result, a comparison between the images produced by these fluoroandrogens and those produced by FDG was of interest.

The images realized using fluorolabeled androgens vs FDG are reported by Larson et al. Variations in lesion uptake were noticed. Certain cervical lesions that were detected using ^{18}F MDHT were virtually undetected using ^{18}F -FDG. The variations in these scans may be attributed to several reasons, one of which is the variability in the ligand binding domain of AR between different cell lines.

Certain prostate cancer cell lines contain a mutation in the ligand binding domain(LBD) of AR²³. A T877A mutation is seen in the LBD in the androgen receptor of LNCaP/C4-2 cells²⁰. This mutation of a threonine to alanine reduces steric strain and increases the lipophilicity of the AR binding pocket. Studies have shown that the effects of various androgens are different on cells expressing wild-type AR and cells expressing mutant AR⁵. The mutations in the AR binding pocket may be a reason why the use of different PET ligands causes variability in the images produced. Additionally, studies have shown that these ligands can be competitively displaced by circulating androgens^{11,18,21,22}.

The variability in the images produced when using different ligands is of interest to our group. This chapter focuses on the study of intratumoral androgen synthesis. Our group investigates the effects of DHT precursors on AR activation. An understanding of this mechanism in prostate cancer may provide guidance into the development of other imaging agents that may provide a more accurate and comprehensive image of the disease in vivo.

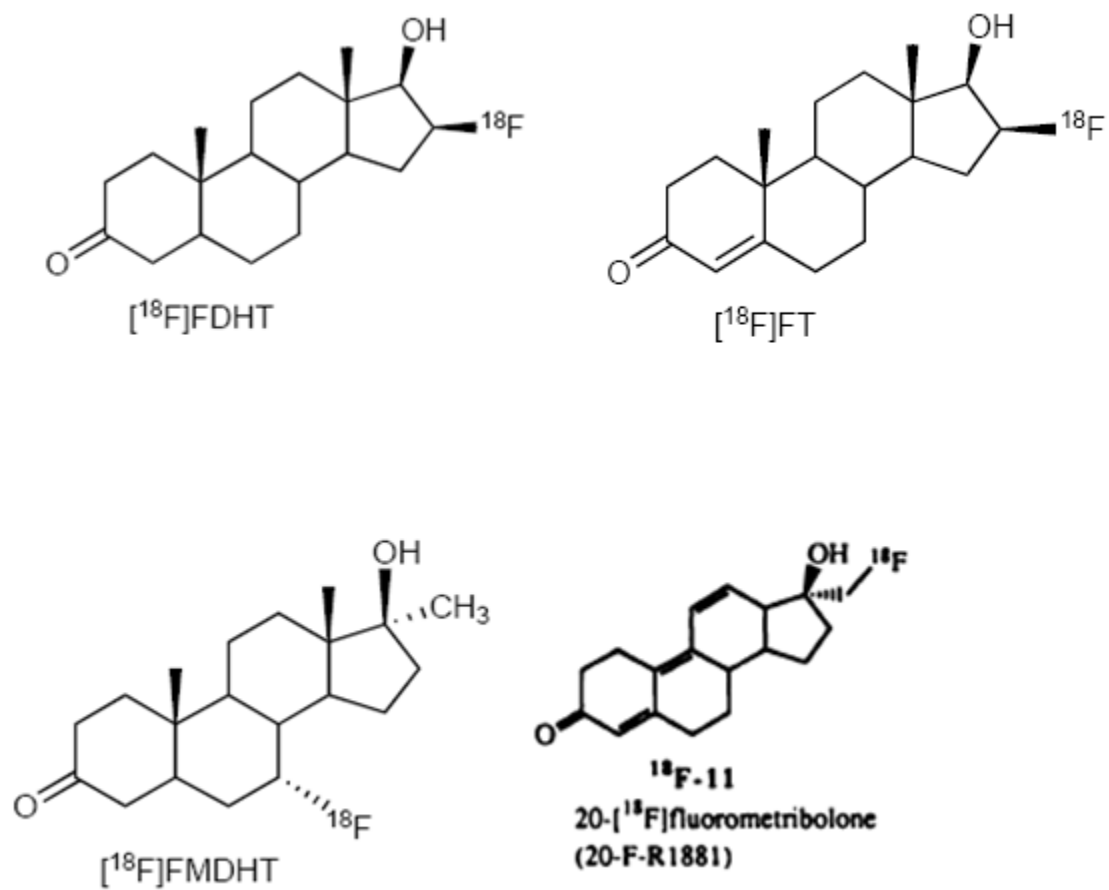


Figure 2.1: Fluorolabeled Androgen Derivatives

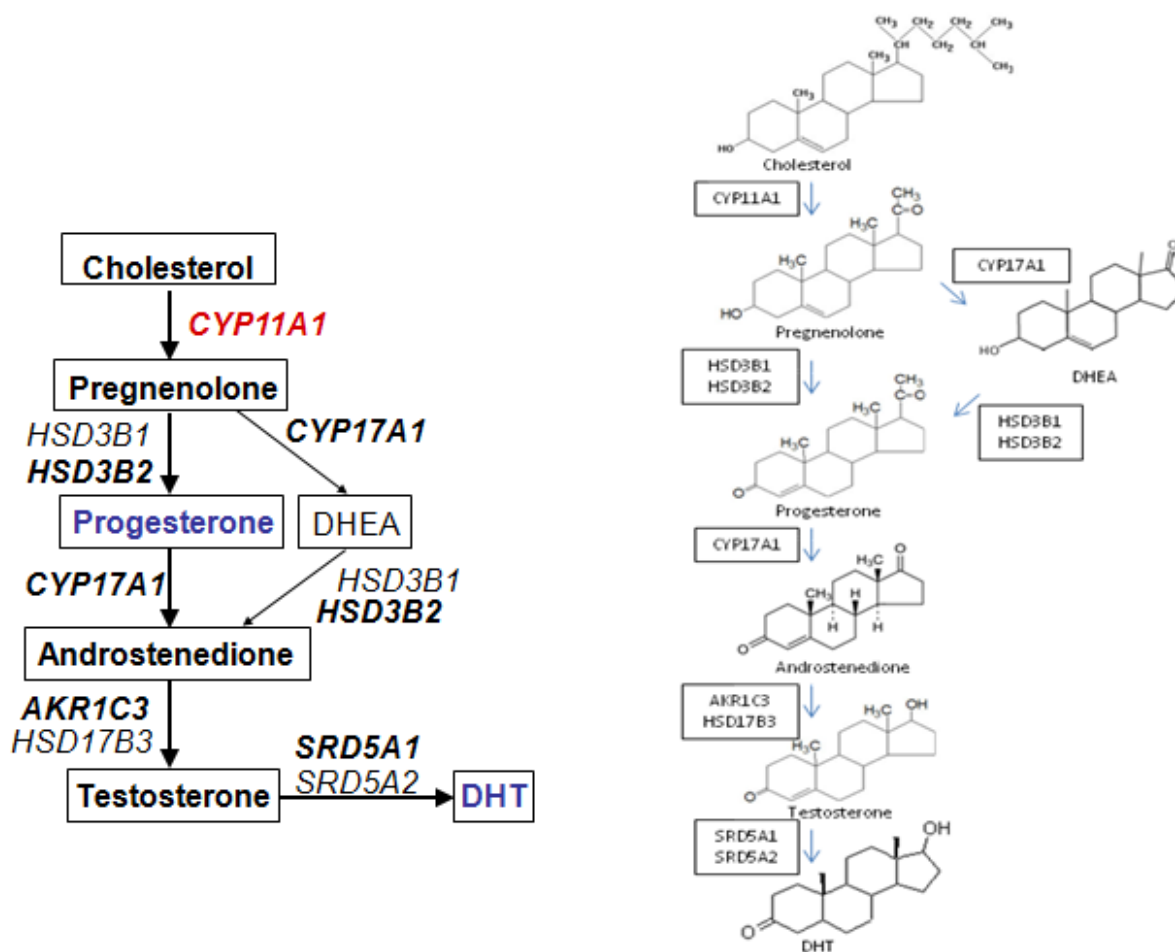


Figure 2.2: Androgen Synthesis Pathway

2.2: Experimental

General Procedure Cell Culture:

C4-2 (T877A Mutant AR) and VCap (Wild-type AR) cells were cultured in RPMI1640 medium with 10% FBS containing 1 mL Gentamycin. Cells were grown to 80-90% confluence and were then subjected to trypsin digest and washed with PBS buffer. Cells were plated in 12 well plates using 5% charcoal/dextran-stripped FBS (CSS) media and allowed to settle for 24 hours. After 24 hours, cells were treated with appropriate androgen or drugs. Cells were incubated at 37°C and 5% CO₂ environment for 24 hours.

General Procedures for Harvesting of Protein Samples:

Upon completion of designated incubation period, cells were harvested using 200uL of 2% SDS. Lysates were obtained and boiled at 100°C for 15 minutes. Cells were quantified using a Perkin Elmer Wallac Victor3 1420 Multilabel Counter and Bradford reagent. Samples were prepared using appropriate dilutions with Lamellae Buffer (+Beta mercaptoethanol-BME) and boiled at 100°C for 15 minutes.

General Procedures for Western Blotting:

Samples were loaded into 15 well 4-12% gradient gels (Invitrogen). Gels were run for 2 hours at 120 V. Protein was then transferred to nitrocellulose membranes using Bio-Rad

Transblot SD Semidry Transfer cells with 19V power supply for 2 hours. Blots were blocked with 5% milk for 1 hour and incubated with appropriate primary antibodies [anti-PSA (1:1000, Ab-cam, anti-rabbit), anti-AR (1:2000, Santa Cruz), anti-CYP11A1 (1:500, Abnova), anti- β -tubulin (1:1000, Upstate) for 12 hours at 4°C. Blots were washed 4x 15 minutes with TBST solution. Blots were then incubated with appropriate secondary antibodies [(Anti-Rabbit (1:1000), Anti-Mouse (1:1000 (Promega))] for 1 hour at room temperature. Blots were washed 4 x 15min with TBST and developed using autoradiography cassettes and developing reagent.

General Procedures for Lipofectamine™ 2000 Transfection:

Transfection of siRNA samples was performed using Lipofectamine™ 2000 reagent (Invitrogen). Appropriate volumes of Optimem I solution was aliquoted to 1.5mL autoclaved tubes. Appropriate concentrations of siRNA samples were diluted in Optimem I solutions. Lipofectamine™ 2000 was diluted (1:100). Lipofectamine™ 2000 solutions were combined with siRNA samples and were gently mixed and incubated at room temperature for 20 minutes to allow complexes to form. Cells were treated with 200uL of appropriate siRNA solution. Cells were incubated for 72 hours at 37°C and 5% CO₂ environment and harvested.

General Procedures for RT-PCR Experiments:

Quantitative real-time RT-PCR amplification was conducted on RNA extracted from tissue samples or cell lines using TRIZOL reagent. 50ng RNA was used for each reaction and the

result was normalized by co-amplification of 18s RNA. Reactions were performed on ABI Prism 7700 Sequence Detection System using Taqman one-step RT-PCR reagents.

2.3: Results/Discussion

To study the mechanism of the androgen synthesis pathway seen in Figure 2.2, we decided to explore the effects of different androgens on LNCaP cells, a cell line that expresses mutant AR. As seen in Figure 2.3, LNCaP cells were treated with different doses of DHT, progesterone, testosterone and androstenedione. The Western Blots show that there is an upregulation of AR activity seen when LNCaP cells are treated with DHT and Pg and such effects are not as significant when cells are treated with testosterone and androstenedione. This data suggests the activation of AR by progesterone via direct agonist binding.

To further understand the androgen synthesis pathway, studies of the various enzymes involved in converting cholesterol to different androgens were conducted. As a preliminary experiment, samples of bone metastatic tumor CRPC cells were obtained and the mRNA expression of two genes, CYP17A1 and CYP11A1 was determined. As seen in Figure 2.4, there is a negative correlation between the two proteins. CYP17A1 is responsible for converting progesterone to androstenedione, while CYP11A1 is responsible for the conversion of cholesterol to upstream androgens like progesterone. The negative correlation between the two proteins may be indicative of a compensatory effect between the proteins involved in the pathway. A lack of CYP17A1 in viable cells is compensated for by an up regulation of CYP11A1.

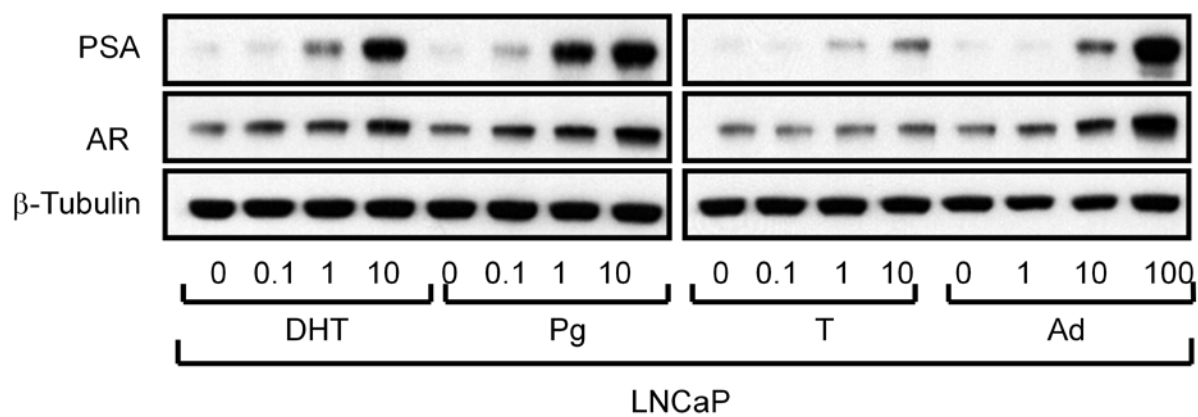


Figure 2.3: Treatment of PCa cell line expressing mutant AR with various androgens

The investigation of the levels of the different enzymes was further developed with mRNA expression experiments of these proteins in different cell lines. The main area of focus here was to study the difference, if any, in the expression of proteins present in different cell lines, mainly cell lines expressing wild-type AR and mutant AR. VCap (Wild-type AR) and C4-2 (Mutant AR) cell lines were used for this experiment. As seen in Figure 2.5, a difference in the levels of the proteins is apparent. The expression of proteins such as CYP17A1, AKR1C3, and HSD13C in VCap cells is significantly higher compared to the expression levels of these proteins observed in C4-2 cells. However, experiments determining CYP11A1 expression show the opposite indicating that C4-2 cells have significantly higher expression of this protein compared to VCap cells. This data may be indicative of efficient activation of mutant AR by other androgens. The lower levels of CYP17A1 and other downstream enzymes in C4-2 cells indicate that DHT and testosterone may not be the only viable androgens serving as agonists to AR. Additionally, the low levels of CYP17A1 in these cells indicate that C4-2 cells may be bypassing the CYP17A1 enzyme when synthesizing androgens.

Furthermore, a higher level of CYP11A1 protein is seen in C4-2 cells as seen in Figure 2.6. Figure 2.6 compares the protein levels of CYP11A1 in different cell lines. The level of the upstream CYP11A1 enzyme is significantly higher in C4-2 cells compared to other cell lines such as LNCaP, RV1, PC3, LAPC4 and VCaP. This data also contributes to the thought of upstream androgens such as progesterone activating mutant AR in PCa cell lines such as C4-2.

In addition to treating cells with androgens, a large number of studies focus on the effects of inhibiting enzymes involved in the androgen synthesis pathway. Our group also decided to

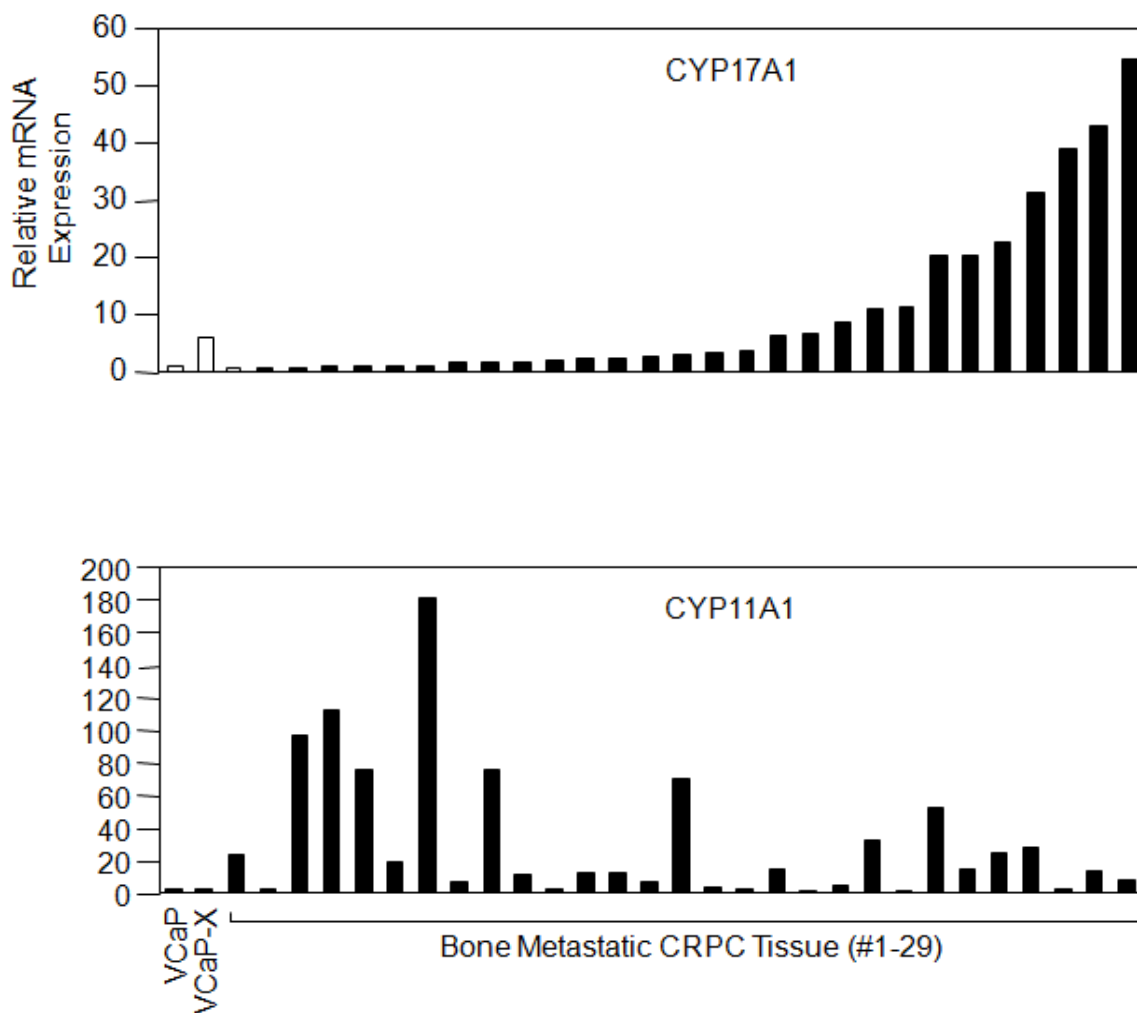


Figure 2.4: mRNA studies of CYP11A1 and CYP17A1 Enzymes in Metastatic CRPC cells

investigate the effects of protein inhibition in this pathway. We decided to study the response of cells when CYP17A1 was knocked down. Two compounds were used to accomplish this inhibition, Abiraterone and Ketoconazole. Both compounds are CYP17A1 inhibitors and Abiraterone is currently in clinical trials. Generally, groups indicate that patients treated with Abiraterone have responded well to the drug. Such groups observed that Abiraterone consistently induced a significant decrease in PSA levels [according to 1 report: (30% reduction 14/21 (66%); 50% reduction 12/21 (57%) and 6 of 21 (29%) with a duration of PSA responses: 69 to 1578 days²] and a reduction in tumor size²⁸. As seen in Figure 2.7, Abiraterone has an androgen scaffold while Ketoconazole does not. In the Western Blots seen in Figure 2.8, Abiraterone has inhibitory effects on progesterone induced AR activity. Given our hypothesis of progesterone binding directly to AR in C4-2 cells, this down regulation induced by Abiraterone was unexpected. As seen in Figure 2.2 CYP17A1 is downstream from progesterone. If progesterone was in fact directly binding to AR as hypothesized, CYP17A1 inhibition would have no effect on AR activity. If we considered the data present in Figure 2.8 independently, we would conclude that our hypothesis was incorrect and that progesterone does not bind directly to AR. However, upon investigating this further, this may not be the case. Our group designed an experiment to learn more about Abiraterone's effects on PCa. We decided to compare its effects with another CYP17A1 inhibitor, Ketoconazole. We treated C4-2 cells with DHT and then treated with Ketoconazole and Abiraterone. In this experiment, it was expected that either drug would have no effect on DHT induced activity. Again referring to Figure 2.2, CYP17A1 is located upstream compared to DHT. Thus, inhibition of this protein would have no effect on activity upregulated by such an androgen. When analyzing Figure 2.9, it is apparent that Ketoconazole, as expected, has no effect on the DHT induced response. However, inhibition is observed with the treatment

with Abiraterone. To try and explain this unexpected observation, our group decided to analyze the differences between Ketoconazole and Abiraterone. As seen in Figure 2.7, an obvious difference is present in the structures of the molecules. Abiraterone has a structure that resembles androgens such as DHT and Pg. Abiraterone's androgen scaffold makes the drug susceptible to binding the LBD of AR. The inhibition of DHT induced activity by Abiraterone may be indicative of this binding. If bound to AR, Abiraterone would effectively block DHT from binding, causing the inhibition of DHT induced activity seen in Figure 2.9. Additionally, when bound to AR, Abiraterone may have some sort of antagonist effect on the receptor, causing AR to adopt an antagonist conformation. This would result in a decrease in transcription and production of AR regulated proteins.

These studies provide evidence for the ability of different DHT precursors, such as progesterone, to activate mutant AR in C4-2 cells. Progesterone may be directly binding to AR in C4-2 cells, causing an upregulation of AR regulated genes such as PSA. The differences in the LBD of AR and the data summarized above may help to explain why the use of different radio labeled androgens produce different results when metastatic prostate cancer is imaged. Certain tumors may have mutant AR and have a different affinity to the radio tracer used. If this is true, those lesions that remain undetected when using tracers such as fluoro labeled DHT may be detected if fluoro labeled progesterone is used. These studies provide a small window into the different routes of AR activation in C4-2 cells that express mutant AR. In addition, it provides insight into Abiraterone, which may be inhibiting AR activity by both CYP17A1 inhibition and direct binding. Data presented in Figure 2.10b provides further evidence supporting this observation. COS-7 cells were used to host both wild-type AR and AR expressing the T877A

mutation. Abiraterone inhibition of androgen induced activity is observed with wild-type AR. The drug also effectively inhibits DHT induced activity of AR expressing the mutation. However, Abiraterone's antagonist effect on mutant AR activity is not as significant in the presence of progesterone. This observation provides evidence for the high affinity of mutant AR for progesterone. As seen, progesterone has a significant induction of AR activity in cells expressing the T877A mutation. This further indicates that Abiraterone may be directly binding to AR and that the T877A mutation causes AR to have a high affinity for and effective activation by upstream androgens including progesterone. Mechanistically, the two molecules, Abiraterone and progesterone, are in direct competition for the ligand binding domain of AR and that mutant AR has a significantly higher affinity for progesterone compared to its affinity for Abiraterone.

Thus far, the main area of focus of this discussion was around CYP17A1. It continues to be an area of interest in this pathway. However, with the data discussed thus far, and the potential activation of AR by androgens(Pg) upstream to CYP17A1, a study of enzymes further upstream became of interest. Figure 2.10 summarizes an experiment knocking down CYP11A1. The data indicates that a down regulation of CYP11A1 causes a decrease in androgen induced AR activity in C4-2 cells, but does not affect the basal levels. This supports the importance of conversion of cholesterol to progesterone in C4-2 cells, further suggesting direct binding of this androgen to AR in PCa cell lines containing an AR mutation.

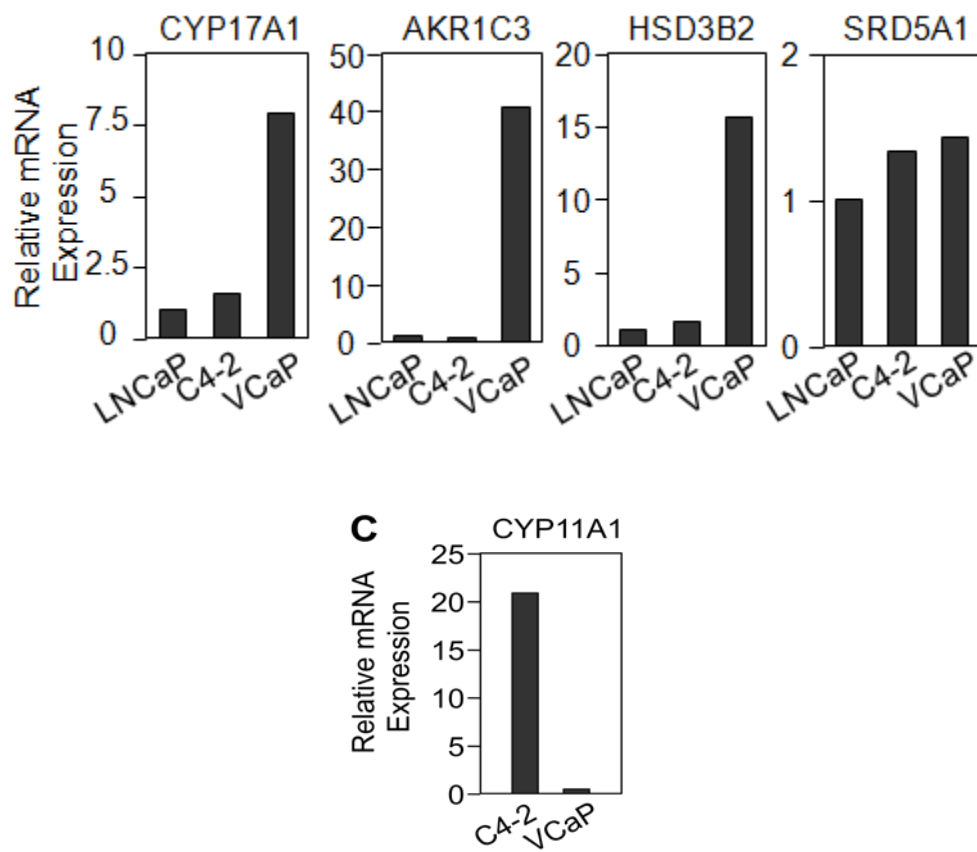


Figure 2.5: mRNA Expression of Proteins Involved in Androgen Synthesis

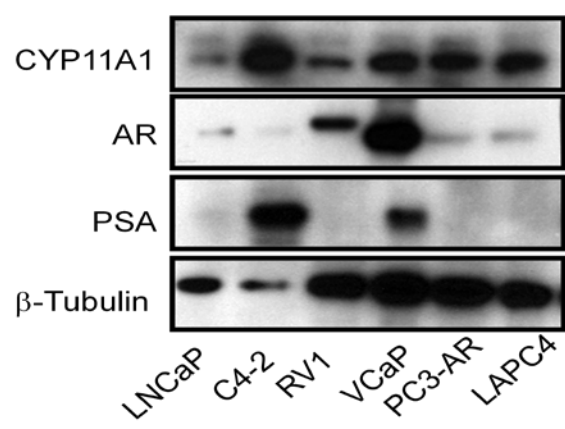
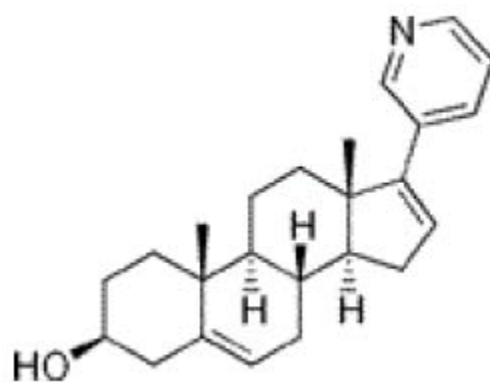
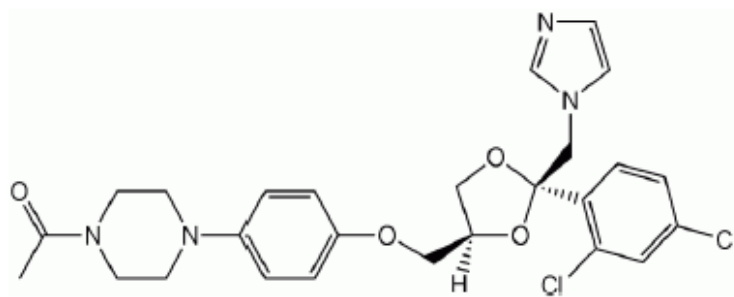


Figure 2.6 : Comparison of CYP11A1 Protein Levels in Different Cell Lines



Abiraterone



Ketoconazole

Figure 2.7: Structures for CYP17A1 Inhibitors Abiraterone and Ketoconazole

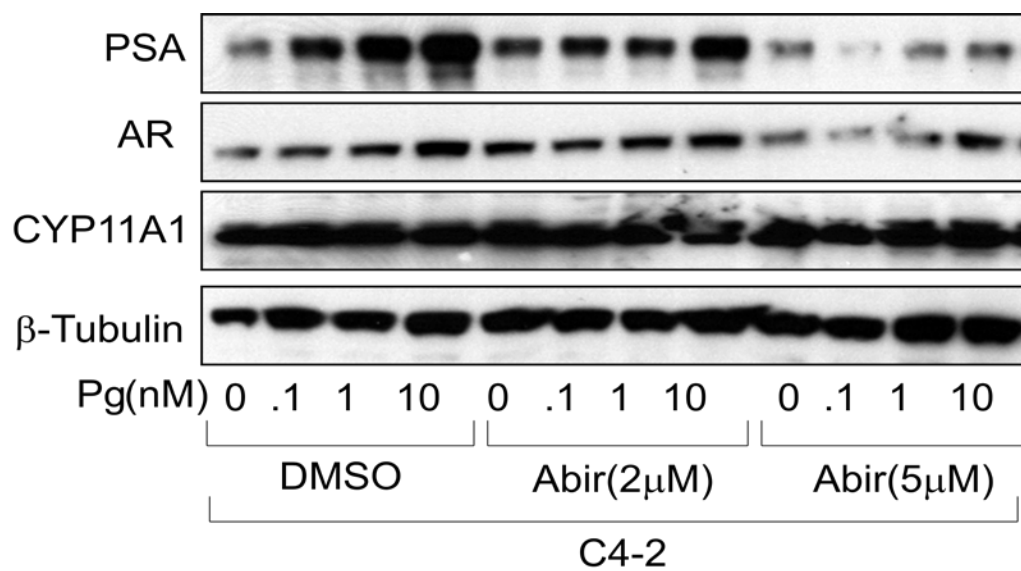


Figure 2.8: Western Blot of C4-2 Cells treated with Abiraterone and Progesterone for 24 hours

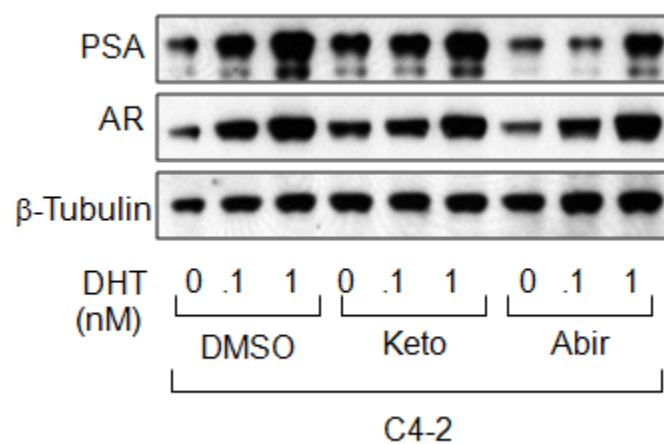


Figure 2.9: Western Blot of C4-2 Cells Treated with DHT, Ketokonazole and Abiraterone for 24 hrs

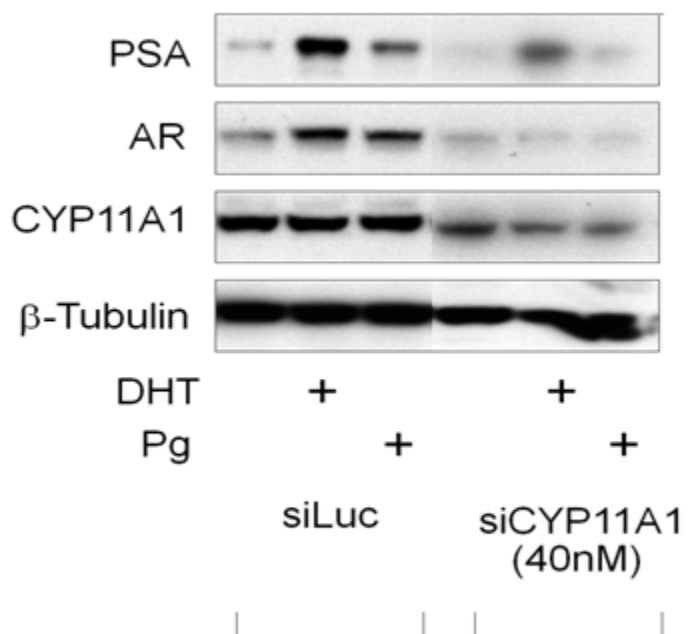


Figure 2.10: Preliminary siRNA CYP11A1 experiment

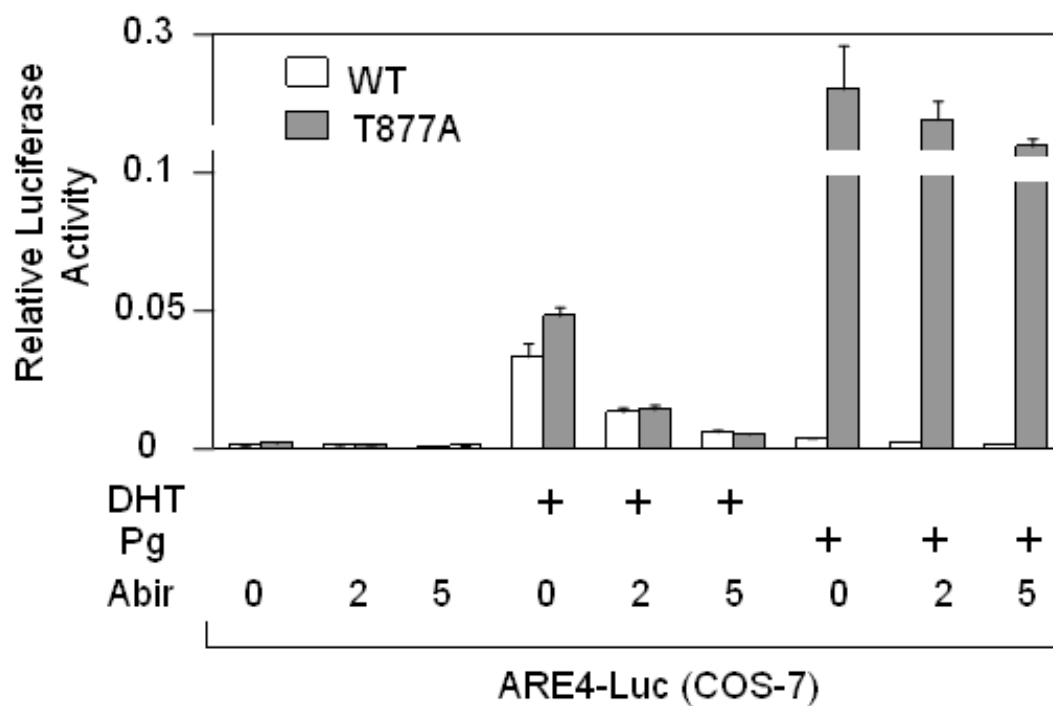


Figure 2.10b: Luciferase Assay Comparing Androgen Induced activity of Wild-Type(WT) and Mutant AR and the Effects of Abiraterone (Conducted by Nick Simon-BIDMC, Boston, MA)

2.4: Future Directions

With this data, several future routes may be explored. Primarily, studies of the androgen synthesis pathway will be continued. Upstream enzymes involved in the pathway, such as CYP11A1, are not well studied. Understanding the role and effects of this enzyme may provide insight into the mechanisms involved in AR reactivation and in the progression of prostate cancer (PCa) to CRPC. Additionally, it may help to determine why patients treated with Abiraterone respond well at first but are not completely cured of the disease.

Currently, there are no known inhibitors of CYP11A1. As a result, knocking down the enzyme to observe its effects on PCa cell lines remains as a challenge. Our group hopes to perform a stable transfection of CYP11A1 siRNA into C4-2 cell lines to knock down CYP11A1 and observe the effects on AR activity and stabilization. Such transfections may be achieved via LipofectamineTM 2000 transfection or through the use of a lentivirus.

In addition to observing the effects of knocking down single enzymes involved in androgen synthesis, our group has preliminarily explored the effects of knocking down two enzymes at a time. For example, we have preliminary data suggesting a synergistic effect with the treatment of cells with Indomethacin (Figure 2.11) and Abiraterone, which inhibit AKR1C3 and CYP17A1 respectively. Figure 2.12 indicates that a combination treatment results in a significant decrease in AR activity. As observed in Figure 2.12, there is a significant down regulation of PSA and other AR regulated genes (ERG) when a combination treatment is administered. However, a significant feedback response is observed with the noteworthy increase in CYP17A1 mRNA expression (Figure 2.12).

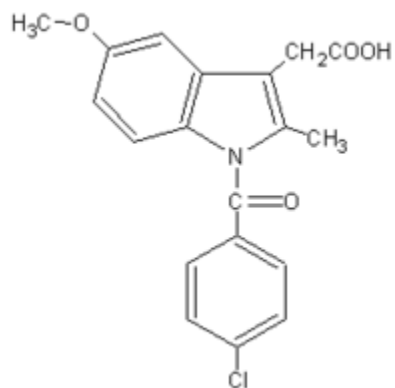


Figure 2.11: Indomethacin, non-steroidal anti-inflammatory drug (NSAID) shown to have inhibitory effects on AKR1C3 in PCa

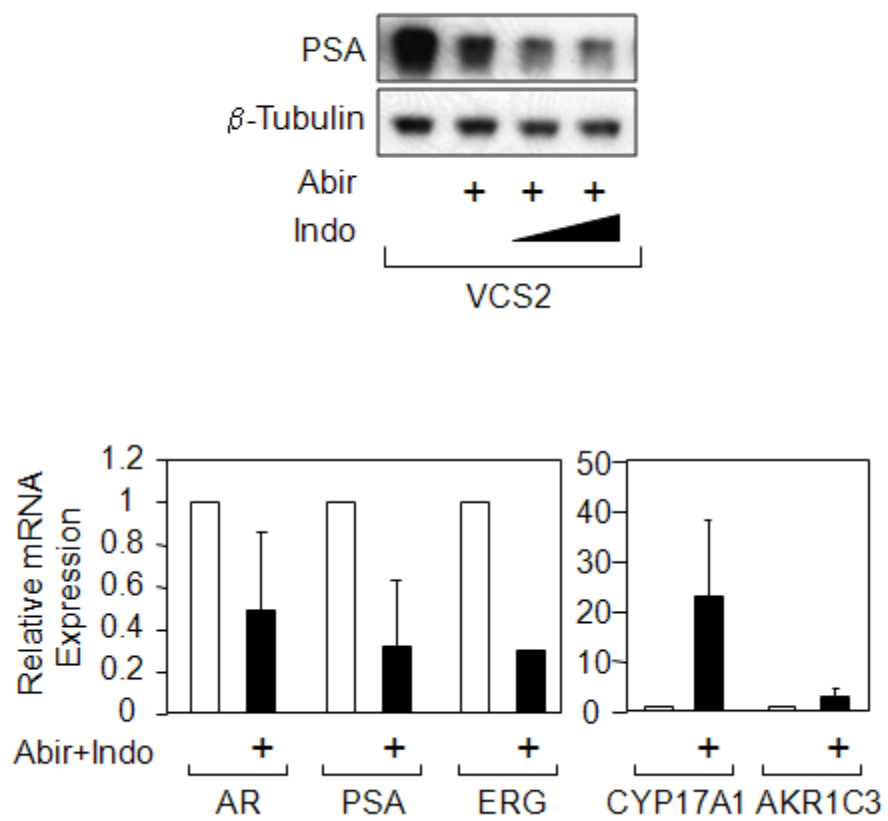


Figure 2.12: Combination Treatment of Abiraterone and Indomethacin

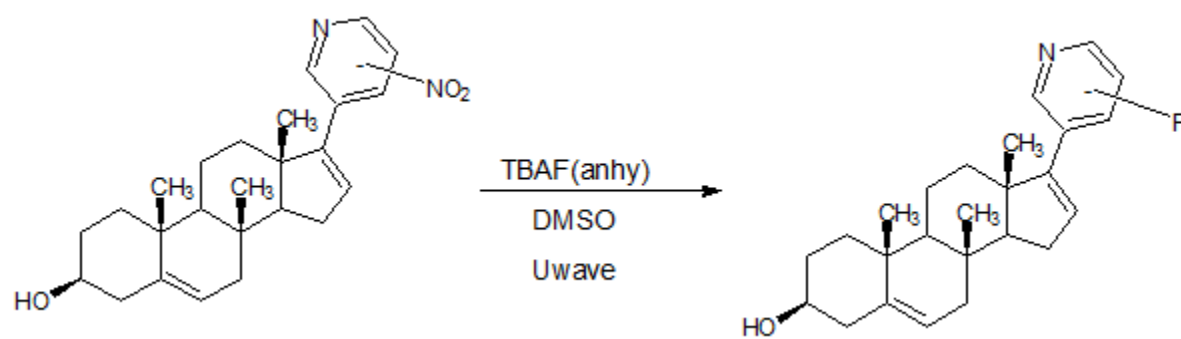
This data suggests the need for further development of combination treatments. The observed upregulation of CYP17A1 mRNA expression with the Abiraterone/Indomethacin combination treatment is significant. It is indicative of cells trying to compensate for the effects of Abiraterone/Indomethacin treatment. With further understanding of this observation, the development of a CYP11A1 inhibitor may be desired. Our group has most recently become interested in knocking down CYP11A1 through various methods, as mentioned above, to determine its effects on AR regulated genes, but an inhibitor is yet to be reported. In essence, the data suggests that the complete androgen synthetic pathway (Figure 2.2) is essential in wild-type AR, because ligands such as DHT and testosterone are most effective in AR activation. However, as seen with mutant AR in LNCaP/C4-2 cells, other androgens, such as progesterone, are effective in inducing AR activity. In these cells, the whole androgen synthesis pathway may not be essential. A high level of CYP17A1 in these cells is not needed. Other enzymes (CYP11A1) play a more vital role in the activity of mutant AR. With these interpretations, a more effective treatment for CRPC may be realized if a synergistic effect is observed with the tandem knockdown of CYP11A1 and CYP17A1. Such a combination treatment could effectively, and more comprehensively, shut down the synthetic pathway (Figure 2.2) providing a more potent treatment for CRPC.

Upon further understanding of the androgen synthesis mechanism, fluorolabeling different molecules targeting AR may be conducted. The data above provides us with some information that suggests that AR may be directly binding to molecules other than DHT and testosterone. With this information, fluorolabeling of different compounds such as progesterone and Abiraterone may be of interest. Abiraterone may be accessible through the microwave

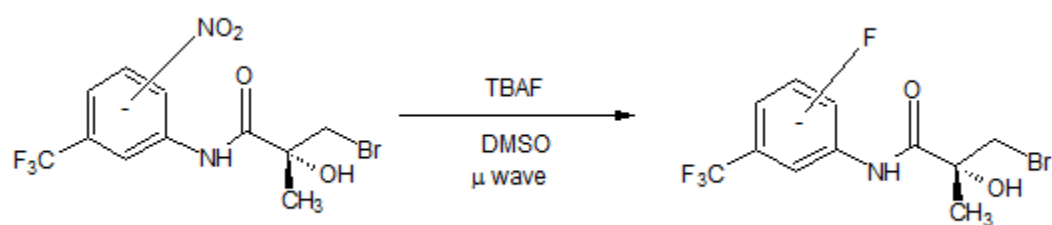
accelerated fluorodenitration methodology described in Chapter 1 because of its pyridine moiety attached to the D ring of the compound. Such a synthesis is proposed in Scheme 2.1 below.

Additionally, further possible fluorolabeling of prostate cancer PET imaging ligands beyond androgens may be explored. Studies labeling non-androgen PET imaging ligands for prostate cancer have been reported. Jacobson et al. reports the use of flutamide derivatives for prostate imaging. With the aromatic ring present in the molecule, flutamide may be accessible via fluorodenitration methods reported by our group as well¹⁶ (Scheme 2.2). The exploration of non-androgenic PET ligands may be investigated on this basis to expand the applications of the chemistry developed and summarized in Chapter 1.

The application of this labeling technique to prostate cancer ligands has a potential two fold benefit: 1) Applications of this methodology may provide a more efficient and accessible means to obtain comprehensive and accurate images of the prostate cancer and 2) Such expedited and versatile techniques can help monitor and track circulating androgens to evaluate the effectiveness of DHT and testosterone precursors on AR activation. The work summarized in this thesis provides some insight into these potential applications, but a deeper understanding of both areas is required to provide a more directed pursuit of these prospective areas of study.



Scheme 2.1: Potential Synthetic Route to Fluorolabeled Androgen



Scheme 2.2: Possible Expedited Route to non-androgenic Fluorolabeled PCa Imaging Ligands
(Flutamide derivatives)

References:

1. Amling, C.L., Prostate-specific antigen and detection of prostate cancer: What we have learned and what should we recommend for screening? *Curr. Treat options Oncol.* **2006**, 7, (5): 337-45.
2. Attard, G.; Beldegrun, A.S.; De Bono, J.S. Selective Blockade of Androgenic Steroid Synthesis by Novel Lyase Inhibitors as Therapeutic Strategy for Treating Metastatic Prostate Cancer. *Urological Oncology*, **2005**, 96: 1241-46
3. Attard, G.; Reid, A.H.M.; Bono, J.S. Selective Inhibition of CYP17 With Abiraterone Acetate is Highly Active in Treatment of Castration-Resistant Prostate Cancer, *Journal of Clinical Oncology*, **2009**, 27(23): 3742-3748.
4. Bonasera, T.A.; O'Neil, J.P.; Jeffrey, M.X.; Dobkin, J.A.; Cutler, P.D.; Lich, L.L.; Choe, Y.S.; Katzenellenbogen, J.A.; Welch, M.J. Preclinical Evaluation of Fluorine-18-Labeled Androgen Receptor Ligands in Baboons, *J. Nucl. Medicine*, **1996**, 37:1009-1015
5. Cai, C.; Chen, S.; Ng, P.; Chen, S.; Balk, S.P. De Novo Androgen Synthesis Reactivates Androgen Receptor in Castration-Resistance Prostate Cancer, *In Press*
6. Edwards J, Krishna NS, Grigor KM, Bartlett JM. Androgen receptor gene amplification and protein expression in hormone refractory prostate cancer. *Br J Cancer*; **2003**, 89: 552–6
7. Ghanadian R.; Waters S.L.; Chisholm, G.D. Investigations into the Use of Br-labeled 5 α -dihydrotestosterone for Scanning the Prostate. *Eur J Nucl Med.* **1977**, 2:155-157
8. Hellerstedt BA, Pienta KJ. The current state of hormonal therapy for prostate cancer. *CA Cancer J Clin.* **2002**, 52 154–79
9. Hillie, U.E.; Hu, Q.; Vock, C.; Negri, M.; Bartels, M.; Muller-Vieria, U.; Lauterbach, T.; Hartman, R.W. Novel Cyp17 inhibitors: Synthesis, biological evaluation, structure-activity relationships and modeling of methoxy- and hydroxy-substituted methyleneimidazolyl biphenyls, *European Journal of Medicinal Chemistry*, **2009**, 44:2765-2775.

10. Hospers, G.A.P.; Helmond, F.A.; Vries, E.G.E.; Dierckx, R.A.; Vries, E.F.J. PET Imaging of Steroid Receptor Expression in Breast and Prostate Cancer, *Curr. Pharm. Design*, **2008**, 14: 3020-3032
11. Hoyte, R.M.; Rosner, W.; Hochberg, R.B. Synthesis of 16-[125]Iodo-5 α -dihydrotestosterone and Evaluation of its Affinity for the Androgen Receptor. *J Steroid Biochem.* **1982**, 16:621-628
12. Huggins C, Hodges CV. Studies on prostatic cancer. I. The effect of castration, estrogen and androgen injection on serum phosphatases in metastatic carcinoma of the prostate, *Cancer Res.* **1941**, 1: 293-7
13. Jacobson, O.; Bechor, Y.; Icar, A.; Novak, N.; Birman, A.; Marom, H.; Fadeeva, L.; Golan, E.; Leibovitch, I.; Gutman, M.; Even-Sapir, E.; Chisin, R.; Gozin, M.; Mishani, E. Prostate Cancer PET bioprobes: Synthesis of F18-radiolabeled hydroxyflutamide derivatives, *Bioorg. & Med. Chemistry*, **2005**, 13: 6195-6205.
14. Jemal A.; Murray T.; Samuels A.; Ghafoor A.; Ward E.; Thun MJ. Cancer Statistics, 2003. *Cancer J Clin.* **2003**, 53:5-26
15. Karr, J.P.; Wajsman, Z.; Madajewics, S.; Kirdani, R.Y.; Murphy, G.P.; Sandberg, A.A. Steroid Hormone Receptors in the Prostate. *J Urol.* **1979**, 122:170-175
16. LaBeaume, P.; Placzek, M.; Daniels, M.; Kendrick, I.; Ng, P.; McNeel, M.; Afroze, R.; Alexander, A.; Thomas, R.; Kallmerten, A.E.; Jones, G.B. Microwave-accelerated fluorordenitrations and nitrodehalogenations: expeditious routes to labeled PET ligands and fluoropharmaceuticals, *Tetrahedron Letters*; **2010**, 51: 1906-1909
17. Larson, S.M.; Morris, M.; Gunther, I.; Beattie, B.; Humm, J.L.; Akhurst, T.A.; Finn, R.D.; Erdi, Y.; Pentlow, K.; Dyke, J.; Squire, O.; Bornmann, W.; McCarthy, T.; Welch, M.; Scher, H. Tumor Localization of 16B-F18-Fluoro-5a-Dihydrotestosterone Versus F18-FDG in Patients with Progressive, Metastatic Prostate Cancer, *Jour. Of Nucl. Med.* **2004**, 45(3):66-373
18. Liu, A.; Dence, C.S.; Welch, M.J.; Katzenellenbogen. Fluorine-18-Labeled Androgens: Radiochemical Synthesis and Tissue Distribution Studies on Six Fluorine-Substituted Androgens, potential Imaging Agents for Prostate Cancer, *The Journal of Nuclear Medicine*; **1992**, 33(5)

19. el-Shirbiny, A.M. Prostate specific antigen, *Adv. Clin. Chem.* **1994**; 31, 99-133
20. Mobbs B.G.; Johnson, I.E.; Connolly, J.G. The Effect of Therapy on the Concentration and Occupancy of Androgen Receptors in Human Prostatic Cytosol. *The Prostate*, **1980**, 31:37-51
21. Mobbs, B.G.; Johnson, I.E. Increased Androgen Binding Capacity in Experimental Prostatic Carcinomas Treated with Estrogen. *Prog. Cancer Research Therapy*, **1984**, 31:467-476
22. Mohler JL, Gregory CW, Ford OH 3rd *et al.* The androgen axis in recurrent prostate cancer. *Clin Cancer Res.* **2004**, 10:440–8
23. Montgomery, B.R.; Mostaghel, E.A.; Vessella, R.; Hess, D.L.; Kalhorn, T.F.; Celestia, H.S.; True, L.D.; Nelson, P.S. Maintenance of Intratumoral Androgens in Metastatic Prostate Cancer: A Mechanism for Castration-Resistant Tumor Growth, *Cancer Research*; **2008**, 68(11): 4447-4454
24. Oh WK. The evolving role of estrogen therapy in prostate cancer. *Clin Prostate Cancer*, **2002**, 1 : 81–9
25. Osterline, J.E., Prostate specific antigen: a critical assessment of the most useful tumor marker for adenocarcinoma of the prostate. *J Urol*, **1991**, 145(5): 907-23
26. Small EJ, Halabi S, Dawson NA *et al.* Antiandrogen withdrawal alone or in combination with ketoconazole in androgen-independent prostate cancer patients: a phase III trial (CALGB 9583). *J Clin Oncol.* **2004**, 22: 1025–33
27. Tindall DJ. Androgen receptor (AR) coregulators: a diversity of functions converging on and regulating the AR transcriptional complex. *Endocr. Rev.* **2007**, 28 (7): 778–808.
28. www.advancedprostatecancer.net
29. www.organic-chemistry.org